

Ternary fission of α -structured nuclei with $12 \leq A \leq 60$: A three-body decay approachC. Karthikraj^{1,*} and Zhongzhou Ren^{1,2,†}¹*School of Physics Science and Engineering, Tongji University, Shanghai 200092, China*²*Key Laboratory of Advanced Micro-Structure Materials, Ministry of Education, Shanghai 200092, China*

(Received 12 February 2020; accepted 17 July 2020; published 7 August 2020)

We study the ternary fission of various even-even α -structured parent nuclei with $12 \leq A \leq 60$, such as ^{12}C , ^{16}O , ^{20}Ne , ^{24}Mg , ^{28}Si , ^{32}S , ^{36}Ar , ^{40}Ca , ^{44}Ti , ^{48}Cr , ^{52}Fe , ^{56}Ni , and ^{60}Zn , within a three-body decay approach. In the present study, we consider the three spherical ternary fission fragments with the lightest fragment A_3 at the middle of the other two main fission fragments, A_1 and A_2 . The effects of hyperradius and the hypermomentum quantum number in the ternary fission potential energy barrier are also studied. Further, the total excitation energy and the ternary fission relative yields are calculated for the possible ternary fragmentation of each parent nuclei considered. From the results obtained, we find the emission of α -structured ternary fragments is more favored than the other ternary fragment combinations.

DOI: [10.1103/PhysRevC.102.024607](https://doi.org/10.1103/PhysRevC.102.024607)**I. INTRODUCTION**

There has recently been considerable renewed interest in the study of nuclear ternary fission (TF) since it has a larger energy release than in the conventional binary fission process. The term “ternary fission” refers to the breakup of a nucleus into three fragments and is known as an exotic process because of its very low occurrence compared to binary decays. Generally, the exotic TF process can happen in three different ways, i.e., two direct fission modes (equatorial, referring to orthogonal emission, and collinear, referring to polar emission) and one cascade fission mode. The TF process is often referred to as light-charged-particle-accompanied (LCP-accompanied) fission since the third fragment is very light and, in most cases, is an α particle emitted in a direction perpendicular to the main fission fragments. Interestingly, a new kind of phenomenon of the emission of three fragments with similar masses was reported in the recent experimental studies [1,2] and the authors called this exotic decay mode “collinear cluster tripartition.” In addition, the ternary emission probability in thermal-neutron-induced and spontaneous fission of different heavy radioactive nuclei, such as $^{235}\text{U}(n_{\text{th}}, f)$ [3–5], $^{241}\text{Pu}(n_{\text{th}}, f)$ [6], $^{249}\text{Cf}(n_{\text{th}}, f)$ [7,8], and $^{252}\text{Cf}(sf)$ [4,5,8–15] have been reported within the framework of various theoretical models and different experimental techniques. Further, the TF of superheavy and hyperheavy ($Z \geq 126$) nuclei was also studied [16–18], using different theoretical approaches. Overall, the recent experimental studies [1,2] and the various theoretical model predictions [10,11,19–21] suggest that the collinear configuration is preferred relative to the equatorial configuration. However in Ref. [22], the authors showed from general principles that direct collinear fission is improbable.

Within the statistical approach of a two-step binary process, Andreev *et al.* [9] studied the TF charge distribution for the spontaneous fission of ^{252}Cf and induced fission of ^{56}Ni , which was formed in the reaction $^{32}\text{S} + ^{24}\text{Mg}$ at a large angular momentum and an excitation energy of about 84 MeV. Further, they obtained a good comparison with the experimental data for the TF yields of ^{56}Ni with ^8Be and ^{12}C as third particles. In Refs. [23,24], Oertzen *et al.* experimentally studied the binary fission and coplanar ternary cluster decay of hyperdeformed ^{56}Ni and ^{60}Zn formed in the reactions $^{32}\text{S} + ^{24}\text{Mg}$ and $^{36}\text{Ar} + ^{24}\text{Mg}$, respectively, and obtained the double differential cross-section data for the ternary decay with third fragment missing charges from 2 to 8. The authors reported that the ternary decay with third fragment missing charge 2 has the largest yield value than the other measured TF channels.

Royer *et al.* [20,25–28] studied the potential energy barriers for the TF of ^{36}Ar , ^{40}Ca , ^{44}Ti , ^{48}Cr , ^{56}Fe , and ^{56}Ni within a rotational liquid drop model taking into account the nuclear proximity energy and found the TF barrier heights were competitive with the binary ones at high angular momenta. Further, the energies of the ^8Be , ^{12}C , ^{16}O , ^{20}Ne , ^{24}Mg , and ^{32}S nuclei have been studied [29,30], within an α -particle model approach. The authors assumed different planar and three-dimensional shapes of the α molecules (linear chain, triangle, square, tetrahedron, pentagon, trigonal bipyramid, square pyramid, hexagon, octahedron, octagon, and cube) and found that the binding energies of the three-dimensional shapes at the contact point were higher than the ones of the planar configurations. Further, they reported that the core + α cluster configuration leads always to the lowest potential energy barrier.

The binding energy per nucleon as a function of the nuclear mass number shows a large deviation for light nuclei with maximal value for the α -structured nuclei, especially for ^4He , ^8Be , ^{12}C , and ^{16}O , which indicates a strong preference of α

*c.karthikraj@gmail.com

†zren@tongji.edu.cn

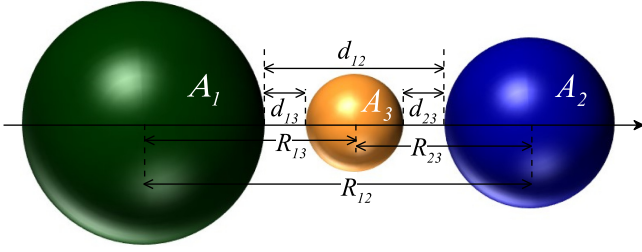


FIG. 1. Schematic illustration of the emission of the three spherical fragments in a three-body decay. Here the lightest fragment A_3 is kept at the center of the other two fission fragments, A_1 and A_2 . The center-to-center distances R_{ij} and the surface separation distances d_{ij} are also labeled. The horizontal solid arrow line represents the fission axis.

clustering in the nucleosynthesis of these elements as well as the heavier ones. The clustering phenomenon, which is an important ingredient in nuclear dynamics, has long been known from the earlier studies on α -cluster models by Wheeler [31] and Hafstad and Teller [32]. A recent review on cluster models can be found in Ref. [33]. The effects of four body interactions of α particles on properties of nuclear α particle condensates in heavy self-conjugate nuclei was studied in Ref. [34] and a quartet model approach [35] was proposed to study α clustering. Using this approach, the authors calculated the numerical results of nuclear radius and α -cluster formation probability for ^{20}Ne , ^{44}Ti , and ^{212}Po nuclei and obtained good agreement with the experimental data and other theoretical model results. Further, they reported that their proposed approach could help in deepening the understanding of α clustering across the nuclide chart.

The aim of this paper to study the total excitation energy and the ternary fission yields and/or charge distribution of fragments from the TF of different parent nuclei with $12 \leq A \leq 60$. The organization of the paper is as follows: A brief description of the theoretical approach used in our calculations is given in Sec. II. The calculations and results are discussed in Sec. III. Finally, the summary of our results and conclusions is given in Sec. IV.

II. THEORETICAL APPROACH

In the present study, the ternary fission is assumed to occur in a single step, i.e., direct decay. Further, the ternary fission fragments are considered to be in spherical shape. Figure 1 represents the schematic illustration of the spherical ternary fragments with the lightest fragment A_3 kept in the middle of the other two fragments, A_1 and A_2 .

To study the exotic ternary decay process within the three-body decay approach, we parameterized the system using a quantity called hyperradius (ρ) which depends on the masses of each fragment m_i and their distance R_{ij} . It is defined as

$$\rho \equiv \sqrt{\frac{1}{mM} \sum_{i < j}^3 m_i m_j R_{ij}^2}, \quad (1)$$

where $M = \sum_{i=1}^3 m_i$, m is an arbitrary normalization mass taken as equal to the nucleon mass, and R_{ij} is the center-to-center distance between the interacting fragments, i and j . $R_{ij} = R_{ij}^t + d_{ij}$, where R_{ij}^t is the sum of the radii of fragments, i and j , and d_{ij} is the surface separation distance between the fragments. The radius of each fragment is calculated as $R_x = 1.2536A_x^{1/3} - 0.80012A_x^{-1/3} - 0.0021444/A_x$ fm [36] with $x = 1, 2$, and 3 corresponding to three fragments A_1, A_2 , and A_3 . The surface separation distances for the ternary configuration presented as in Fig. 1 are considered as $d_{13} = d_{23} = d$ and $d_{12} = 2(R_3 + d)$, and $d = 0$ refers the touching configuration.

A particular decay orientation is defined by the positive scaling factors S_{ij} and it can be calculated as

$$S_{ij}^2 \equiv \frac{R_{ij}^2}{\rho^2}. \quad (2)$$

For example, $S_{13} = S_{23} = S_{12}$ represents the equatorial emission with three identical fragments and $S_{13} + S_{23} \approx S_{12}$ the ternary decay proceeds through a linear chain as depicted in Fig. 1.

The total potential energy $V(\rho)$ of the ternary fission fragments is considered as the sum of the Coulomb potential V_C , nuclear potential V_N , and the centrifugal potential V_K and is given by

$$V(\rho) = V_C + V_N + V_K. \quad (3)$$

The Coulomb interaction energy defines the force of repulsion between the three fragments and it can be parameterized by the hyperradius and scaling factors [37] as

$$V_C = \sum_{i < j}^3 \frac{Z_i Z_j e^2}{R_{ij}} = \frac{1}{\rho} \sum_{i < j}^3 \frac{Z_i Z_j e^2}{S_{ij}}, \quad (4)$$

and the centrifugal potential is defined as in Ref. [37],

$$V_K = \frac{\hbar^2(K + 3/2)(K + 5/2)}{2m\rho^2}, \quad (5)$$

where K is the hypermomentum quantum number.

For the calculation of nuclear interaction potential V_N between the three spherical fragments, we have used the form given in Ref. [8] defined as

$$V_N = \sum_{i < j}^3 V_{ij}^N \{d_{ij}[R_{ij}, R_i, R_j]\}, \quad (6)$$

with

$$V_{ij}^N \{d_{ij}[R_{ij}, R_i, R_j]\} = \frac{v_1 C + v_2 C^{1/2}}{1 + \exp\left[\frac{d_{ij}}{(d_1 + d_2)/C}\right]}, \quad (7)$$

where $v_1 = -27.190 \text{ MeV fm}^{-1}$, $v_2 = -0.93009 \text{ MeV fm}^{-1/2}$, $d_1 = 0.78122 \text{ fm}$, $d_2 = -0.20535 \text{ fm}^2$, and $C = \frac{R_i R_j}{R_i + R_j} \text{ fm}$. In this paper, the TF potential barrier is calculated as a function of hyperradius of the three fission fragments [see Fig. 2(a) for the ternary decay of ^{60}Zn]. The top and bottom of the potential barrier are defined as V_{\max} and V_{\min} , respectively, and the quasifission potential barrier (B_{qf}) is calculated as the difference of potential energies between V_{\max} and V_{\min} . The

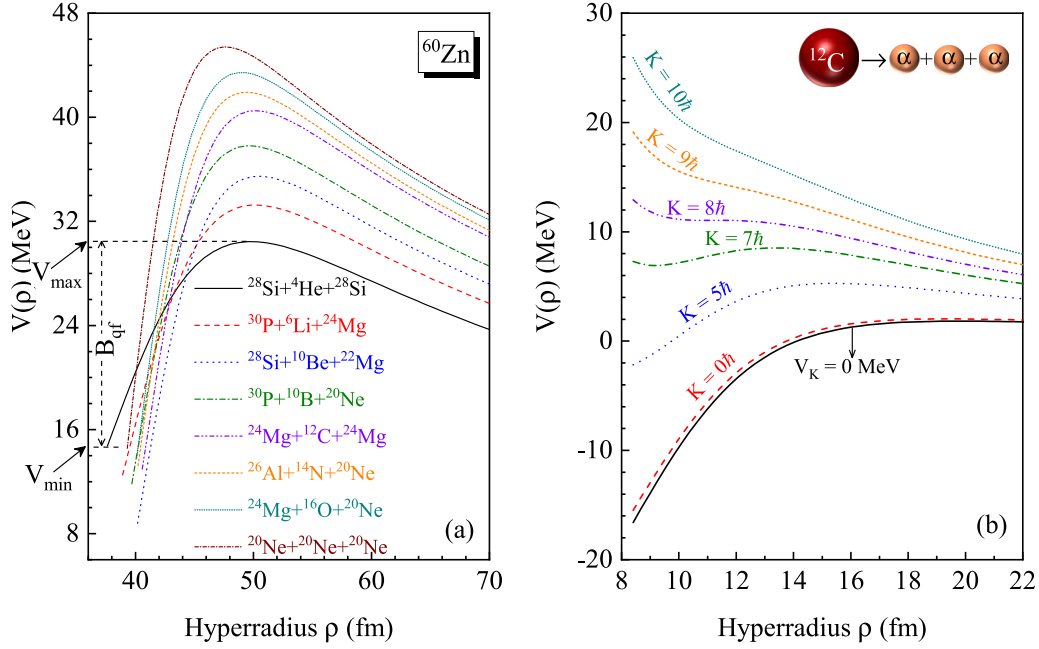


FIG. 2. The x axis is the hyperradius (ρ in fm) of the ternary system as defined in Eq. (1) and the y axis is the total potential energy [$V(\rho)$ in MeV] as a function of hyperradius, which can be calculated from Eq. (3). (a) Potential energy barrier as a function of hyperradius of the ternary fragments from the ternary fission of ^{60}Zn . Different lines correspond to the various charge combinations of the ternary fragments and we labeled them in the order of considered fragment geometry, i.e., $A_1 + A_3 + A_2$. The top (V_{\max} in MeV) and bottom (V_{\min} in MeV) of the potential barrier and its height (B_{qf} in MeV) are also labeled. (b) Variation of potential energy barrier as a function of the hypermomentum quantum number (K in \hbar) and the hyperradius (ρ in fm) for the emission of 3α particles from ^{12}C decay. The solid line corresponds to $V_K = 0$ MeV and the other lines refer to different K values.

height of the potential barrier decreases with increasing K , which is presented in Fig. 2(b) for the decay of ^{12}C into 3α particles.

The total excitation energy (E_{tot}^*) of three fission fragments is related to the Q value of the ternary fission reaction as follows:

$$E_{\text{tot}}^* = \xi_f^* + Q - V_{\min}. \quad (8)$$

Here ξ_f^* is the excitation energy of the fissioning parent nucleus and we consider $\xi_f^* = 50$ MeV. Further, the Q value of the ternary fission reaction can be calculated as

$$Q = \sum_{i=1}^3 \text{BE}_i - \text{BE}_f, \quad (9)$$

where BE_i ($i = 1, 2, \text{ and } 3$) and BE_f are the ground-state binding energies of the three fission fragments and the fissioning nucleus, respectively, which are taken from Ref. [38].

The relative ternary fission yield, $Y(A_i, Z_i)$, of a particular ternary system with given masses and charges of the ternary fragments is statistically calculated as follows:

$$Y(A_i, Z_i) = Y_0 P(A_i, Z_i) W(A_i, Z_i), \quad (10)$$

where the formation probability $P(A_i, Z_i)$ can be calculated as in Ref. [39],

$$P(A_i, Z_i) = P_0 \exp\left[-\frac{U}{T_f}\right], \quad (11)$$

and the decay probability $W(A_i, Z_i)$ can be found as in Ref. [39],

$$W(A_i, Z_i) = W_0 \exp\left[-\frac{B_{\text{qf}}}{T_\eta}\right]. \quad (12)$$

In Eqs. (10), (11), and (12), Y_0 , P_0 , and W_0 are normalization factors for the corresponding distributions. Here $U = V_{\min} - Q$ is called the driving potential of the ternary system. T_f and T_η are correspond to the temperature values of the fissioning compound nucleus and the ternary system, respectively: $T_f = \sqrt{\xi_f^*/a}$ and $T_\eta = \sqrt{E_{\text{tot}}^*/a}$, where $a = A/8$ is the level density parameter with A is the mass number of the fissioning nucleus. In Eq. (12), the term $\exp[-B_{\text{qf}}/T_\eta]$ accounts the thermal penetration of the decay barrier.

Finally, for the calculation of ternary fission charge distribution, the following expression is used:

$$\mathcal{Y}(Z_i) = \mathcal{Y}_0 \max[Y(A_j, Z_i)], \quad (13)$$

where \mathcal{Y}_0 is the normalization factor. From the above Eq. (13), for a certain set of Z_i (i.e., Z_1, Z_2 , and Z_3) the maximum yield is identified over different sets of A_j (i.e., A_1, A_2 , and A_3). In this study, all the distributions and the yields are normalized to unity. Further, it is to be noted that our yield results are limited only to prompt disintegration of a parent nucleus into three fragments.

III. RESULTS AND DISCUSSION

In the present paper, the ternary fission of different even-even α -structured parent nuclei ^{12}C , ^{16}O , ^{20}Ne , ^{24}Mg , ^{28}Si , ^{32}S , ^{36}Ar , ^{40}Ca , ^{44}Ti , ^{48}Cr , ^{52}Fe , ^{56}Ni , and ^{60}Zn are studied within a three-body decay approach. It is to be noted that the above-considered nuclei are negative Q -value systems and, hence, would decay if they were produced in heavy-ion reactions with sufficient compound nucleus excitation energy, which is taken here as $\xi_f^* = 50$ MeV. Further, we consider the three fission fragments are in spherical shape and the fragment A_3 is also assumed at the middle of the other two fragments, A_1 and A_2 .

A. Total excitation energy

For the considered α -structured parent nuclei, the possible ternary fission fragment configurations with the third fragment not lighter than ^4He are generated by the use of AME2016 data. The procedure for the generation of all possible ternary fragment combinations is already described in Refs. [15,40]. For thus-generated ternary fragment combinations, the potential energy barrier among the three fission fragments is calculated as a function of hyperradius (ρ in fm) of the ternary system, using Eq. (3) and the ternary fission reaction Q value is also calculated from Eq. (9). In Fig. 2(a), the calculated potential energy barrier, for different possible charge combinations of the ternary fragments from the ternary decay of ^{60}Zn , is presented as a function of hyperradius (ρ). From this figure, it is found that the height of the potential barrier decreases with the increase of charge asymmetry of the ternary fragments. The top and bottom of the potential barrier are also mentioned for the $^{28}\text{Si} + ^4\text{He} + ^{28}\text{Si}$ fragmentation. In Fig. 2(b), the variation of potential barrier with respect to the hypermomentum quantum number (K in \hbar) and ρ is presented for the ternary decay of ^{12}C into 3α particles. The potential barrier corresponds to $V_K = 0$ MeV is also shown. From this figure, it is seen that there is no potential barrier from $K = 8\hbar$ onward. Further, the height of the potential barrier decreases with the increase of K values.

The total excitation energy E_{tot}^* is calculated for the possible ternary combinations of each considered α -structured parent nuclei, using Eq. (8). To identify the maximal E_{tot}^* value from each ternary charge combination of a parent system, a two-dimensional minimization approach [15,40] is used. In which the minimization of the possible ternary fragment combinations with respect to the charge number (Z_1 , Z_2 , and Z_3) of the ternary fragments has been carried out. In Fig. 3, the maximal E_{tot}^* of spherical fragments from the ternary fragmentation of different nuclei are presented in ternary contour plots as a function of the charge numbers of the proton minimized ternary fragments. The total excitation energy results presented in this figure are due to $K = 0\hbar$. Different Figs. 3(a)–3(k) correspond to the maximal E_{tot}^* of the charge minimized ternary fragments from the ternary fragmentation of various parent nuclei, such as ^{20}Ne , ^{24}Mg , ^{28}Si , ^{32}S , ^{36}Ar , ^{40}Ca , ^{44}Ti , ^{48}Cr , ^{52}Fe , ^{56}Ni , and ^{60}Zn , respectively. The proton magic numbers are also shown here as dashed lines to see the importance of closed-shell effects. For ^{12}C ternary decay, the

emission of 3α particles has pronounced the largest E_{tot}^* value than the other possible ternary fragmentation of the parent system. Further, it is worthwhile to mention that the emission of 3α particles in triangular direction is preferred over the collinear type emission, which supports the earlier predictions as well. However, the E_{tot}^* results for the ternary fission of ^{12}C and ^{16}O nuclei are not shown here due to their smaller possibility of fragment combinations. In Fig. 3, the maximal E_{tot}^* is found for the ternary fragmentation which involves $Z_3 = Z_2 = 2$, i.e., ^4He . In addition, the calculated E_{tot}^* for the ternary fragmentation involves the α -structured fragments is larger compared to the other neighboring ternary combination which consists of non- α -structured fragments. This indicates the preference for the emission of α -structured fragments over the non- α -structured fragments. A similar kind of results was already reported in Ref. [41] for the binary fission potential energy studies of $^{56}\text{Ni}^*$.

B. Ternary fission yields

For the possible ternary fragment combinations with $E_{\text{tot}}^* > 0$ MeV of each parent nuclei, the formation and decay probabilities of the ternary fragments are calculated by using Eqs. (11) and (12), respectively. With the use of these two quantities, the relative ternary fission yield is also calculated from Eq. (10). By using a two-dimensional approach, which was mentioned earlier, the maximal yield value of every possible ternary charge combinations (Z_1 , Z_2 , and Z_3) from each parent nuclei is identified. In Fig. 4, the ternary fission charge distribution of different parent nuclei with various possible even-charge third fragments is presented as a function of charge numbers (Z_1 and Z_2) of the accompanying fission fragments. Here different lines with various symbols correspond to yield results due to various possible even-charge third fragments. It is to be noted here that the ternary fission charge distribution due to the other third fragments is also calculated but not presented here because of their smaller significance. Further, it is to be noted that the presented yield results are due to $K = 0\hbar$ only. To show the ternary fission charge distribution results as a function of charge numbers of the accompanying fragments, the calculated yield values are normalized to 2. Similarly to E_{tot}^* , the calculated relative yield results have pronounced the largest values for the emission of 3α particles from the ternary fission of ^{12}C . From the charge distribution results presented in Fig. 4, ternary configurations with $Z_3 = 2$ are shown to have larger yield values than the other possible even-charge third fragment configurations. In particular, the prominent peaking structure is obtained for the ternary fragmentation which involves $Z_3 = Z_2 = 2$. In addition, the calculated relative yield values for a ternary fragmentation which contains the α -structured fragments are larger compared to the other non- α -structured ternary fragments. Note that our calculated ternary fission yield results, for the case of ^{56}Ni , shows larger yield value for $\text{Cr} + \alpha + \alpha$, $\text{Ti} + \alpha + \text{Be}$, $\text{Ca} + \alpha + \text{C}$, $\text{Ar} + \alpha + \text{O}$, $\text{Si} + \alpha + \text{Mg}$ ternary configurations, whereas it has been found for the $\text{Si} + \alpha + \text{Mg}$ ternary combination from the experimental observation [23].

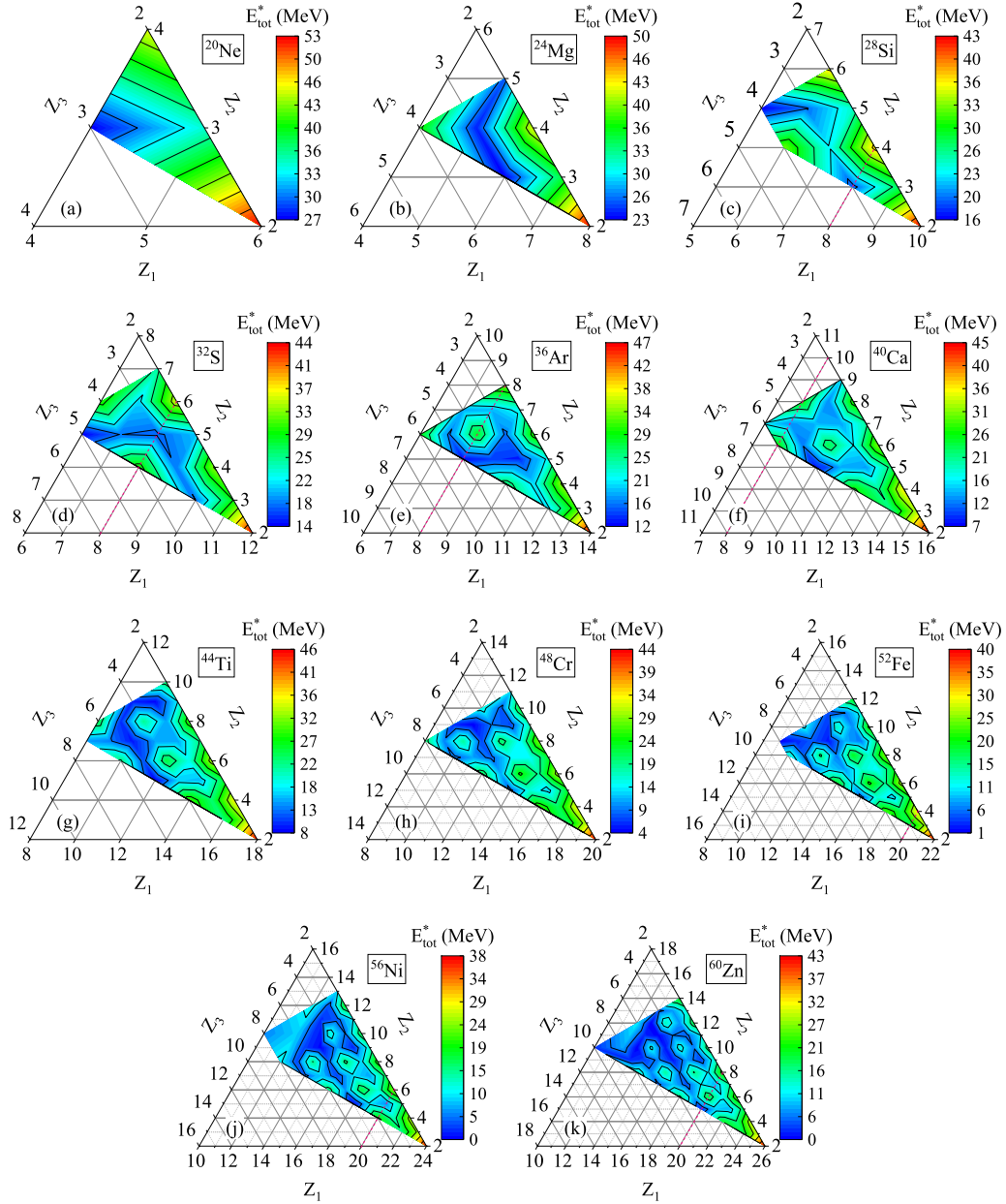


FIG. 3. The total excitation energy E_{tot}^* of charge-minimized (Z_1 , Z_2 , and Z_3) spherical fragments from the ternary fragmentation of different parent nuclei at the excitation energy of $\xi_j^* = 50$ MeV. Panels (a)–(k) correspond to the different parent systems considered. The dashed lines correspond to the proton magic numbers.

IV. SUMMARY AND CONCLUSIONS

Within a three-body decay approach, we have studied the ternary fission of various even-even α -structured parent nuclei with $12 \leq A \leq 60$. In the present study, the ternary fragments are considered to be spherical and the ternary breakup is also assumed to occur in a single stage, i.e., a direct decay into three fragments. For ^{12}C ternary decay, the effects of hyperradius and the hypermomentum quantum number in the ternary fission potential energy barrier are explicitly presented. Note that the total excitation energy E_{tot}^* of the ternary fragments has been calculated from the proper energy conservation in a ternary fission reaction and it is

found to vary as a function of mass and charge numbers of the ternary fragments. Interestingly, for each α -structured parent nuclei, the largest E_{tot}^* is obtained for the ternary fragmentation with $Z_2 = Z_3 = 4$ He. Further, the ternary fragmentation which involves α -structured fragments have larger E_{tot}^* values than the other ternary fragmentation consisting of non- α -structured fragments. This indicates the preference for the emission of α -structured fragments over the other non- α -structured ternary fragments. The effect of strong maxima in the total excitation energy E_{tot}^* for α -structured ternary fragments is also reflected in the ternary fission yields. In other words, the calculated ternary fission yields are larger for the emission of α -structured ternary fragments than the

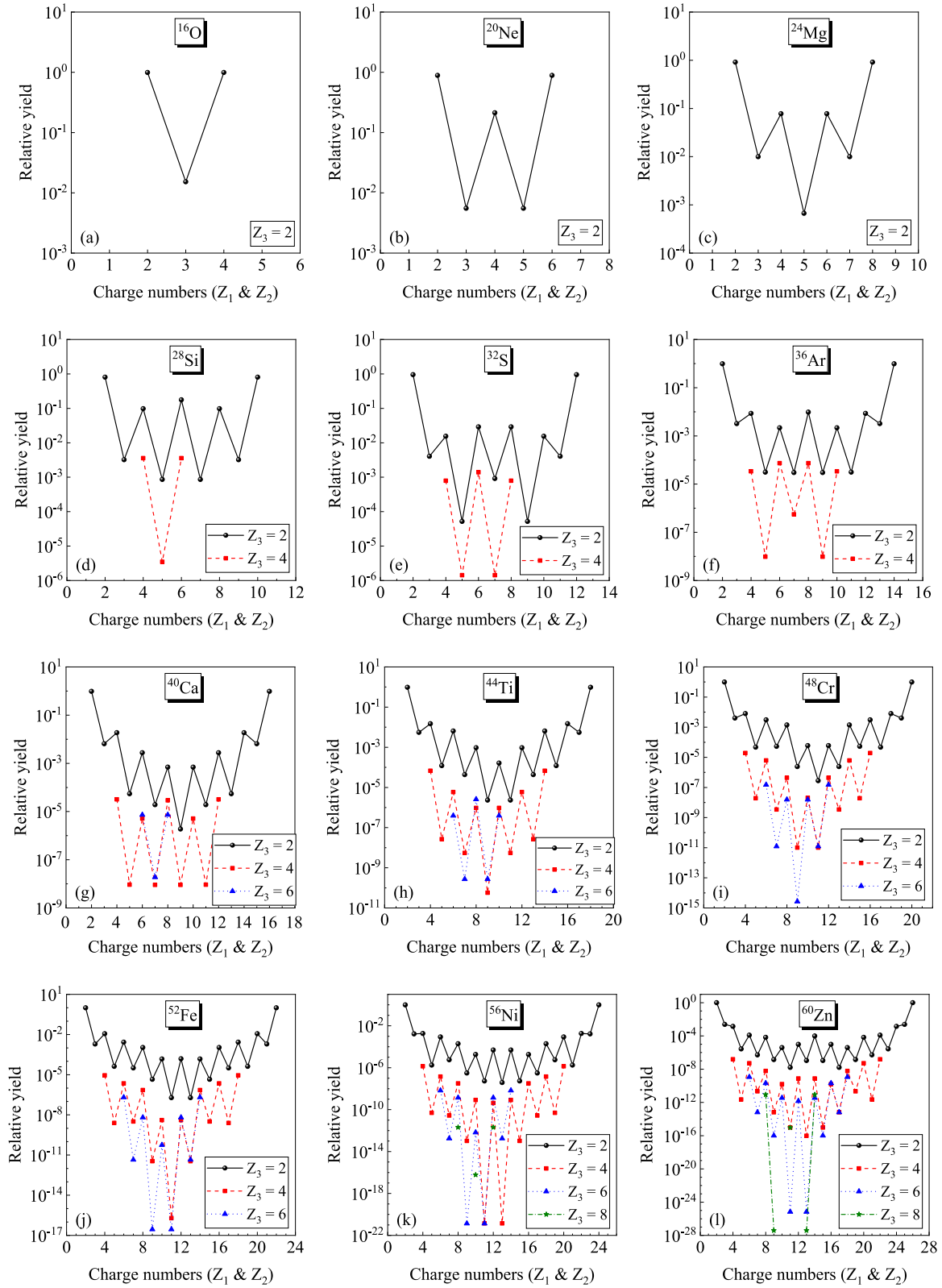


FIG. 4. For different parent nuclei with various possible even-charge (Z_3) third fragments, the ternary fission charge distribution plotted as a function of charge numbers (Z_1 and Z_2) of the accompanying fragments. Different lines with solid symbols represent the relative yield values due to various possible even-charge third fragments. Panels (a)–(l) correspond to the different parent systems considered.

other ternary fragments. In addition, for different parent nuclei with various possible even-charge third fragments, the ternary fission charge distribution results are also presented.

Further, the emission of ternary combinations contain α -structured fragments are shown here as favorable ternary modes to look for from the ternary fission of α -structured nuclei with $12 \leq A \leq 60$, at $\xi_f^* = 50$ MeV. As a future course of study, the effects of deformation and orientation of ternary fragments will be explored within this approach.

ACKNOWLEDGMENTS

The work is supported by the National Natural Science Foundation of China under Grants No. 11975167, No. 11761161001, No. 11535004, No. 11881240623, and No. 11961141003; the National Key Research and Development Program of China under Grants No. 2018YFA0404403 and No. 2016YFE0129300; the Science and Technology Development Fund of Macau under Grant No. 008/2017/AFJ, and the China Postdoctoral Science Foundation under Grant No. 2020M671196.

-
- [1] Yu. V. Pyatkov, D. V. Kamanin, W. von Oertzen, A. A. Alexandrov, I. A. Alexandrova, O. V. Falomkina, N. A. Kondratjev, Yu. N. Kopatch, E. A. Kuznetsova, Yu. E. Lavrova, A. N. Tyukavkin, W. Trzaska, and V. E. Zhuhcko, *Eur. Phys. J. A* **45**, 29 (2010).
- [2] Yu. V. Pyatkov, D. V. Kamanin, W. von Oertzen, A. A. Alexandrov, I. A. Alexandrova, O. V. Falomkina, N. Jacobs, N. A. Kondratjev, E. A. Kuznetsova, Yu. E. Lavrova, V. Malaza, Yu. V. Ryabov, O. V. Strelakovsky, A. N. Tyukavkin, and V. E. Zhuchko, *Eur. Phys. J. A* **48**, 94 (2012).
- [3] R. B. Tashkhodjaev, A. K. Nasirov, and W. Scheid, *Eur. Phys. J. A* **47**, 136 (2011).
- [4] A. K. Nasirov, W. von Oertzen, A. I. Muminov, and R. B. Tashkhodjaev, *Phys. Scr.* **89**, 054022 (2014).
- [5] W. von Oertzen and A. K. Nasirov, *Phys. Lett. B* **734**, 234 (2014).
- [6] U. Köster, H. Faust, G. Fioni, T. Friedrichs, M. Groß, and S. Oberstedt, *Nucl. Phys. A* **652**, 371 (1999).
- [7] I. Tsekhanovich, Z. Büyükmumcu, M. Davi, H. O. Denschlag, F. Gönnewein, and S. F. Boulyga, *Phys. Rev. C* **67**, 034610 (2003).
- [8] V. Yu. Denisov, N. A. Pilipenko, and I. Yu. Sedykh, *Phys. Rev. C* **95**, 014605 (2017).
- [9] A. V. Andreev, G. G. Adamian, N. V. Antonenko, S. P. Ivanova, S. N. Kuklin, and W. Scheid, *Eur. Phys. J. A* **30**, 579 (2006).
- [10] K. Manimaran and M. Balasubramaniam, *Phys. Rev. C* **83**, 034609 (2011).
- [11] K. R. Vijayaraghavan, M. Balasubramaniam, and W. von Oertzen, *Phys. Rev. C* **90**, 024601 (2014).
- [12] M. Balasubramaniam, C. Karthikraj, S. Selvaraj, and N. Arunachalam, *Phys. Rev. C* **90**, 054611 (2014).
- [13] A. V. Karpov, *Phys. Rev. C* **94**, 064615 (2016).
- [14] C. Karthikraj and Z. Ren, *J. Phys. G: Nucl. Part. Phys.* **44**, 065102 (2017).
- [15] C. Karthikraj and Z. Ren, *Phys. Rev. C* **96**, 064611 (2017).
- [16] V. I. Zagrebaev, A. V. Karpov, and W. Greiner, *Phys. Rev. C* **81**, 044608 (2010).
- [17] M. Balasubramaniam, K. R. Vijayaraghavan, and K. Manimaran, *Phys. Rev. C* **93**, 014601 (2016).
- [18] C. Karthikraj, S. Subramanian, and S. Selvaraj, *Eur. Phys. J. A* **52**, 173 (2016).
- [19] H. Diehl and W. Greiner, *Nucl. Phys. A* **229**, 29 (1974).
- [20] G. Royer, F. Haddad, and J. Mignen, *J. Phys. G: Nucl. Part. Phys.* **18**, 2015 (1992).
- [21] D. N. Poenaru, R. A. Gherghescu, and W. Greiner, *Nucl. Phys. A* **747**, 182 (2005).
- [22] T. V. Chuvil'skaya and Yu. M. Tchuvil'sky, *Phys. Rev. C* **99**, 024301 (2019).
- [23] W. von Oertzen *et al.*, *Eur. Phys. J. A* **36**, 279 (2008).
- [24] W. von Oertzen *et al.*, *J. Phys.: Conf. Ser.* **111**, 012051 (2008).
- [25] G. Royer and J. Mignen, *J. Phys. G: Nucl. Part. Phys.* **18**, 1781 (1992).
- [26] G. Royer, *J. Phys. G: Nucl. Part. Phys.* **21**, 249 (1995).
- [27] G. Royer, C. Bonilla, and R. A. Gherghescu, *Phys. Rev. C* **67**, 034315 (2003).
- [28] G. Royer, *J. Phys. Conf. Ser.* **111**, 012052 (2008).
- [29] G. Royer, G. Ramasamy, and P. Eudes, *Phys. Rev. C* **92**, 054308 (2015).
- [30] G. Royer and P. Eudes, *J. Phys. Conf. Ser.* **863**, 012012 (2017).
- [31] J. A. Wheeler, *Phys. Rev.* **52**, 1083 (1937).
- [32] L. R. Hafstad and E. Teller, *Phys. Rev.* **54**, 681 (1938).
- [33] W. von Oertzen, M. Freer, and Y. Kanada-En'yod, *Phys. Rep.* **432**, 43 (2006).
- [34] D. Bai and Z. Ren, *Phys. Rev. C* **97**, 054301 (2018).
- [35] D. Bai, Z. Ren, and G. Röpke, *Phys. Rev. C* **99**, 034305 (2019).
- [36] V. Yu. Denisov, *Phys. Rev. C* **91**, 024603 (2015).
- [37] E. Garrido, D. V. Fedorov, A. S. Jensen, and H. O. U. Fynbo, *Nucl. Phys. A* **748**, 27 (2005).
- [38] M. Wang, G. Audi, F. G. Kondev, W. J. Huang, S. Naimi, and X. Xu, *Chin. Phys. C* **41**, 030003 (2017).
- [39] Sh. A. Kalandarov, G. G. Adamian, N. V. Antonenko, and W. Scheid, *Phys. Rev. C* **82**, 044603 (2010).
- [40] C. Karthikraj and Z. Ren, *Phys. Rev. C* **101**, 014603 (2020).
- [41] C. Karthikraj, N. S. Rajeswari, and M. Balasubramaniam, *Phys. Rev. C* **86**, 014613 (2012).